Science and Technology of
Advanced Materials

Realization of high strength and high ductility for AZ61 magnesium alloy by severe warm working

ELSEVIER

Science and Technology of Advanced Materials 6 (2005) 185–194

SCIENCE AND TECHNOLOGY OF ADVANCED MATERIALS

www.elsevier.com/locate/stam

Realization of high strength and high ductility for AZ61 magnesium alloy by severe warm working

Yu Yoshida, Keita Arai, Shota Itoh, Shigeharu Kamado*, Yo Kojima

Department of Mechanical Engineering, Nagaoka University of Technology, 1603-1, Kamitomioka, Nagaoka, Niigata 940-2188, Japan

Received 14 September 2004; revised 20 October 2004; accepted 24 November 2004

Abstract

Extruded Mg–6%Al–1%Zn (AZ61) alloy bar was subjected to 4-pass Equal Channel Angular Extrusion (ECAE) processing at 448–573 K. At the processing temperature of 448 K, extremely fine grains with the average grain size of 0.5 μm are formed as a result of dynamic recrystallization originated by fine $Mg_{17}Al_{12}$ (β) phase particles having 50–100 nm diameter dynamically-precipitated during ECAE processing. The sizes of both α matrix and β phase decrease with decreasing processing temperatures. In tensile test at room temperature under the strain rate of $1\times10^{-3}\ s^{-1}$, tensile strength increases with decreasing ECAE processing temperatures due to fine grains, fine precipitates and residual strain hardening. Especially, highest strength of 351 MPa was achieved in the specimen ECAE-processed at 448 K. In addition to such high strength, elongation reaches 33% in that specimen. This specimen exhibits clear strain rate dependencies of both flow stress and elongation even at room temperature. As a result, higher elongation of 67% is obtained under low strain rate of $1\times10^{-5}\ s^{-1}$. In such specimen, non-basal slip and grain boundary sliding occur in addition to basal slip. Furthermore, there are grains with no dislocations, suggesting the occurrence of dynamic recovery. The contribution of all the deformation mechanisms would cause high ductility in fine-grained AZ61 alloy specimen with high strength.

Keywords: Equal channel angular extrusion; AZ61 wrought magnesium alloy; Tensile properties; Fine grain; Deformation mechanism

1. Introduction

Demand of magnesium alloys has been increasing remarkably. However, the application of wrought alloys is still limited because of inferior workability of the magnesium alloys having limited slip systems at room temperature. Furthermore, strength of the conventional wrought magnesium alloys is lower than that of aluminum alloys, which prevents application to structural component that requires high strength. It has been reported [1–4] that the strength of magnesium alloys is improved by means of grain refinement according to the Hall–Petch relation. Also, recent research [5–10] reveals that high ductility can be obtained by structure control such as grain refinement and texture control even in magnesium alloys. Recently, Koike et al. [11–13] reported that the ductility is improved in fine-grained magnesium AZ31 (Mg–3 mass%Al–1 mass%Zn) alloys due to the activity of non-basal slip, grain boundary sliding (GBS) and recovery at high strained region. That is, grain refinement improves both strength and ductility in magnesium alloys. Crystallographic orientation also affects the mechanical properties of magnesium alloys. In a previous study, the authors found [7] that the 0.2% proof stress decreases and ductility increases extremely by the application of Equal Channel Angular Extrusion (ECAE) to AZ31 alloy compared with those of the conventionally-extruded specimens. This was because the basal plane of the ECAE-processed alloy is inclined to the extruded direction corresponding to the tensile direction. Therefore, it is expected that both strength and ductility can be improved by means of combining the above severe working process and conventional strengthening methods such as precipitation hardening and work hardening.

* Corresponding author. Tel.: +81 258 47 9710; fax: +81 258 47 9770.
E-mail address: kamado@mech.nagaokaut.ac.jp (S. Kamado).

1468-6996/$ - see front matter © 2005 Elsevier Ltd. All rights reserved.
doi:10.1016/j.stam.2004.11.011

In the present study, Mg–6 mass%Al–1 mass%Zn (AZ61) alloy was subjected to repetitive ECAE processing in order to improve both strength and ductility of magnesium alloy by the refinement of the grains and fine precipitates and by the control of the texture. Relationship between microstructures and tensile properties of ECAE-processed AZ61 alloy were investigated. Furthermore, deformation mechanisms during tensile test were discussed to clarify high ductility of the fine-grained sample.

2. Experimental procedure

Extruded bars of AZ61 alloy were machined into cylindrical specimens having a diameter of 15 mm and a height of 80 mm for ECAE processing. An ECAE die used for the present study has two equal channels of 15 mm diameter [7,8]. The intersecting angle between the two channels is 90° and the angle of the outer arc at the intersection is 60°. Four-pass ECAE processing was carried out in the temperature range from 448 to 573 K. Eight-pass ECAE processing was also performed at 473 K. The 8-pass ECAE specimens were subjected to isochronal annealing at 573, 673 and 773 K for 1 h in order to obtain different grain size. The ECAE specimens were rotated by 90° around the longitudinal axis of the specimen after each pass, which is so-called route B_c, to obtain a homogeneous microstructure.

The microstructure of the specimens was observed using an optical microscope (OM), a scanning electron microscope (SEM) and a transmission electron microscope (TEM). The etching solution was 5% picric acid–13% acetic acid–12% distilled water–70% ethanol mixture for OM observation, and 1% nitric acid–20% acetic acid–19% distilled water–60% ethyleneglycol mixture for SEM observation.

The intensity distribution of the 0002 poles were obtained by a Schulz reflection method [14] utilizing an X-ray diffractometer in order to investigate the texture of the ECAE-processed specimens. The measurement was performed using Cu Kα (wave length $\lambda = 0.15406$ nm) radiation at 50 kV and 300 mA with the sample tilt angle ranging from 0 to 70°.

Tensile tests were carried out at room temperature and at the strain rate of $1 \times 10^{-3}\ s^{-1}$ using as-ECAE-processed specimens. All the tensile direction was parallel to the extrusion direction. Furthermore, specimens ECAE-processed at 448 K were tensile tested with the strain rate ranging from 1×10^{-5}–$1 \times 10^{-1}\ s^{-1}$. The specimens for tensile test were machined to JIS14A tensile specimens, whose gauge length and diameter are 20 and 4 mm, respectively.

The surface of the tensile-tested specimens was observed using a laser microscope and compared to that before tensile test in order to investigate the contribution of GBS to deformation at room temperature. Before tensile test, JIS14B tensile specimen having 20 mm gauge length, 2 mm thickness and 4 mm width was finely polished using 0.05 μm Al_2O_3 suspension. After that, the specimen was elongated up to a given strain, and then the surface of the specimen was observed by a laser microscope.

TEM observation was carried out to investigate the microstructural feature of the deformed specimens. The JIS14B tensile specimens were tested up to a given strain. Subsequently, they were thinned using a handy-wrapping equipment, a dimple grinder and an ion polishing system for TEM observations.

3. Results

3.1. Microstructures

Fig. 1 shows the OM and SEM images of as-received specimen and 4-pass ECAE-processed specimens. Equiaxed grains are uniformly distributed in whole area at each processing temperature due to dynamic recrystallization during ECAE processing. SEM image of as-received specimen reveals some massive $Mg_{17}Al_{12}$ (β) phase along the grain boundaries. In addition to these β compounds, dynamic precipitation of β phase would occur during ECAE processing since solid solubility of aluminum in magnesium solid solution is 6 mass% at 573 K and decreases with lowering temperature. The particle size of the β phase decreases and the number of the particles increases with lowering processing temperature. This may be because of the breakup of the β phase and an increase in the nucleation sites of precipitates by the warm severe working at lower temperatures. Fig. 2 shows correlation between ECAE processing temperature and grain size of 4-pass ECAE-processed specimens. The data of AZ31 alloy obtained in our previous research [7] was also indicated. The grain size decreases linearly with decreasing ECAE processing temperature in both alloys, and that of AZ61 alloy is significantly reduced to about 0.5 μm by repetitive ECAE processing at 448 K. Also, the grain sizes of AZ61 alloy are smaller than those of AZ31 alloy at same temperatures, particularly in a low temperature region. This might be because the numerous fine particles of the β phase in the AZ61 alloy provide nucleation sites for recrystallization.

Fig. 3(a) shows optical micrographs of 8-pass ECAE-processed specimen and after annealing at various temperatures. The grain size increases with increasing annealing temperature as a result of normal grain growth. Fig. 3(b) shows SEM images of specimens annealed at 573 and 673 K. Both Al–Mn compounds and precipitates of β phase are observed in the specimen annealed at 573 K. The precipitates of β phase disappear in the specimens annealed at above 673 K, but Al–Mn compounds still remain. The average grain sizes of the specimens annealed at 573, 673 and 773 K are 2.8, 6.4 and 30.3 μm, respectively.

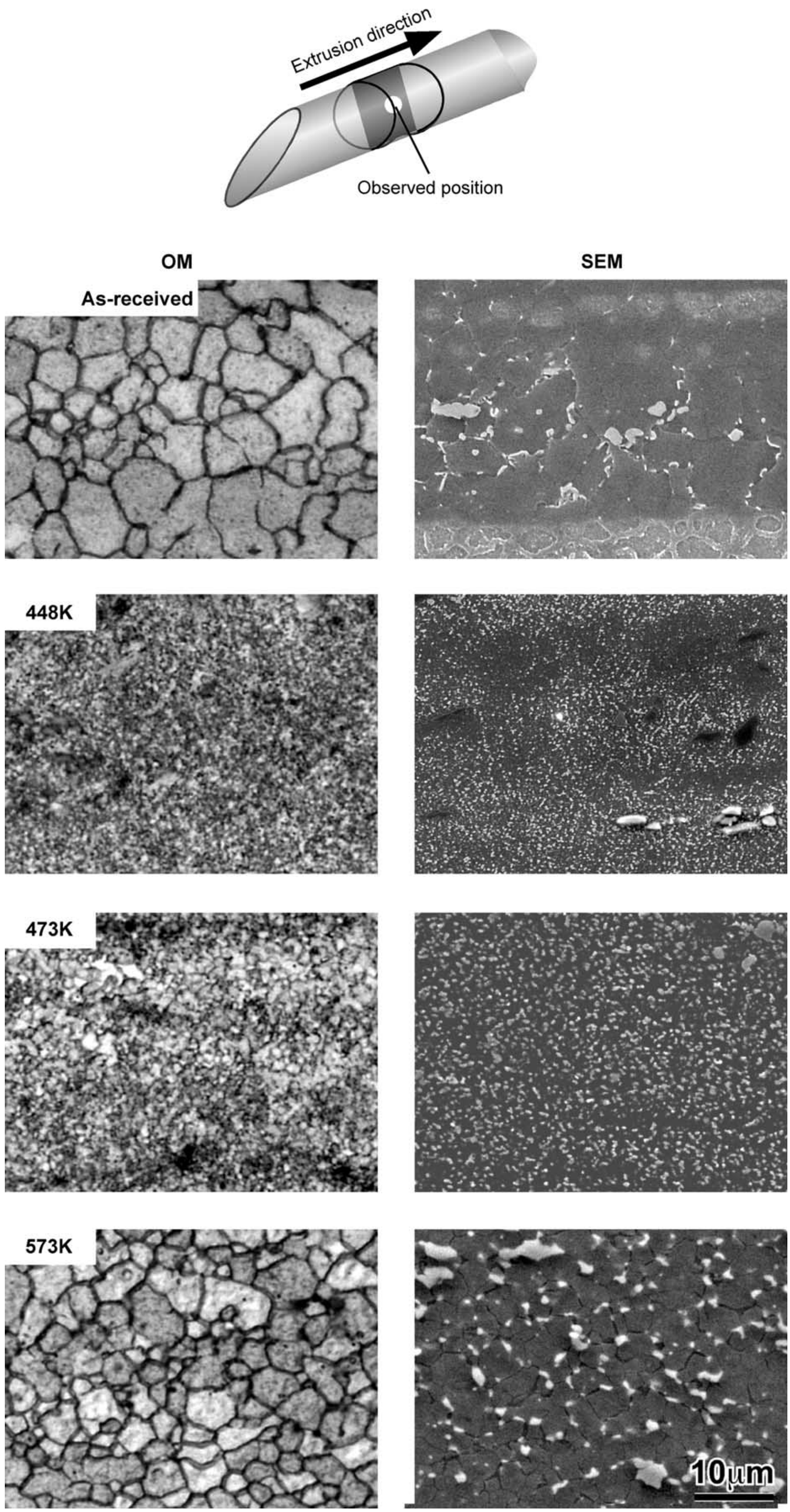

Fig. 1. OM (left) and SEM (right) images of as-received and 4-pass ECAE-processed specimens. ECAE processing temperatures are indicated in the figure.

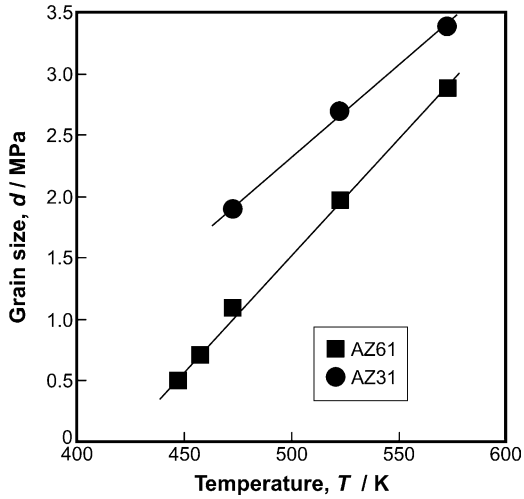

Fig. 2. Correlation between ECAE processing temperatures and grain size of 4-pass ECAE-processed specimens of AZ61 and AZ31 alloys.

Fig. 4 shows TEM image of the specimen ECAE-processed at 448 K. The smallest average grain size of 0.5 μm and the fine β phase having the particle size of less than 100 nm are obtained. Furthermore, few dislocations are visible in the grain interior, suggesting the occurrence of the dynamic recrystallization during ECAE processing. As mentioned above, the AZ61 alloy is remarkably grain-refined compared with the AZ31 alloy. In the AZ61 alloy specimens ECAE-processed at the appropriate temperatures, it is inferred that dislocation pileups around the fine precipitates act as nuclei of recrystallization. Therefore, finer grains are formed in AZ61 alloy comparing with AZ31 alloy that does not precipitate the β phases in the processing temperature range.

Fig. 5 shows the 0002 pole figures of as-received specimen and ECAE-processed specimens. As-received specimen has a texture in which the basal plane is oriented parallel to the extrusion direction and spread toward

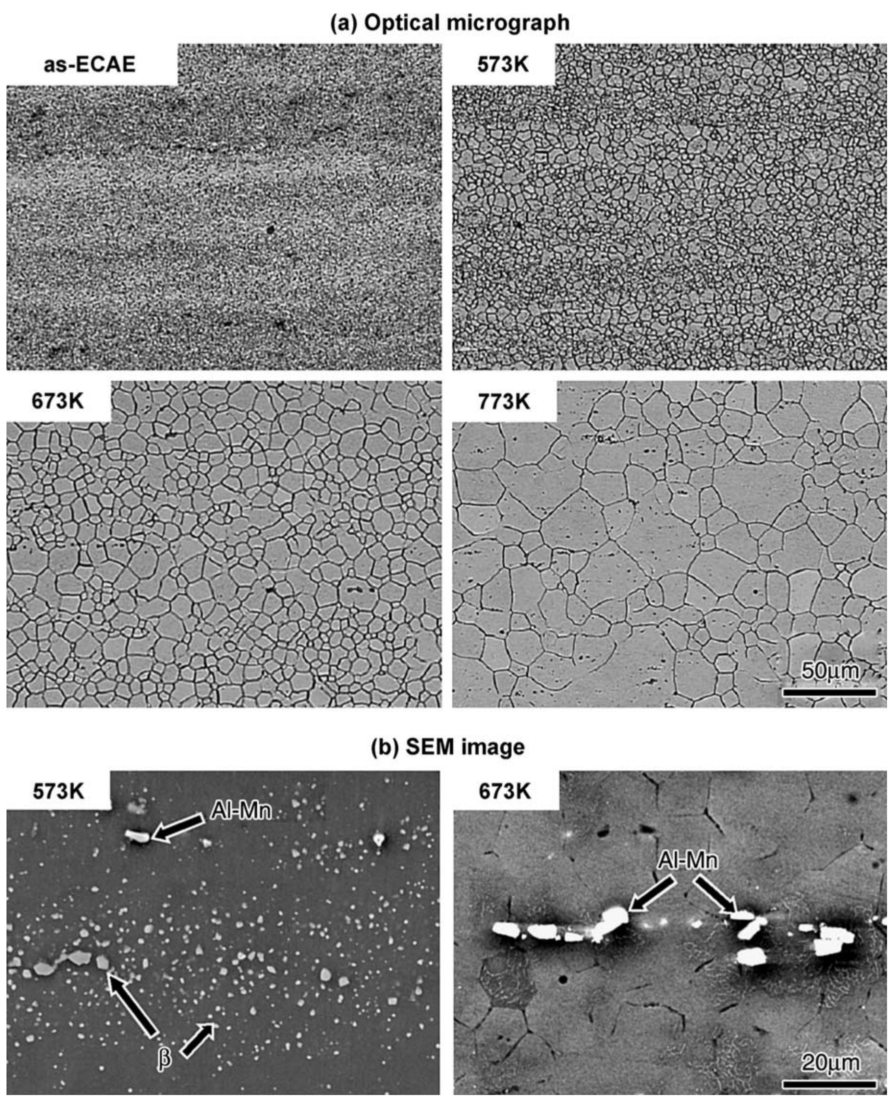

Fig. 3. (a) Optical micrographs of 8-pass ECAE-processed specimen and specimens subsequently annealed at indicated temperatures and (b) SEM images of specimens annealed at 573 and 673 K. Al–Mn compounds and precipitates of β phase are indicated by arrows.

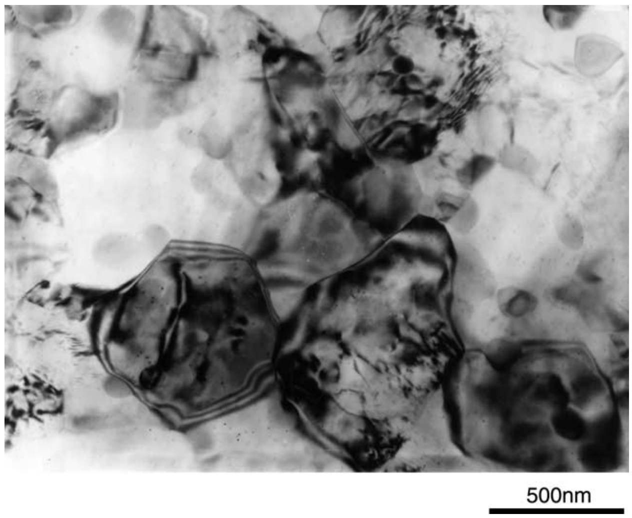

Fig. 4. TEM images of the specimen ECAE-processed at 448 K.

transverse direction of the rod. This is a typical texture in extruded rod of magnesium alloys [1,3,15,16]. After ECAE processing at 448 K, {0002} plane focuses on two orientations in which basal plane is oriented parallel and inclined at 45° to the extrusion direction. The same texture is obtained in the specimen processed at 523 K, while majority of basal plane of the specimen processed at 573 K is oriented parallel to the extrusion direction. The texture of AZ61 alloy formed during ECAE processing differs slightly from that in AZ31 alloy, particularly in the low temperature range. That is, AZ31 alloy ECAE-processed at 473 K has texture in which the basal plane is almost inclined at 45° to the extrusion direction and has few basal planes parallel to the extrusion direction [7].

3.2. Tensile properties

Fig. 6 shows the stress–strain curves of as-received specimen and ECAE-processed specimens. With decreasing ECAE processing temperatures, tensile flow stresses increase, a yielding phenomenon appears and degree of strain hardening after the yielding is lowered. Particularly, the specimen processed at 448 K exhibits tensile strength of 351 MPa, which is higher than that of as-received specimen. An opposite tendency was found in ECAE-processed AZ31 alloy specimens [7], i.e. both tensile and yield strength of the ECAE-processed specimens decrease with decreasing ECAE processing temperature due to appearance of texture in which the basal plane inclined at 45° to the extrusion direction, namely the tensile direction. Generally, such orientation relationship leads to easy slip of basal dislocation, resulting in lowering the strength. Although the AZ61 alloy specimens ECAE-processed at lower temperatures include the grains having inclined basal plane as a part of whole grains, high strength is achieved. This fact means that the significantly fine grains and numerous fine precipitates of β phase as shown in Fig. 1 would be extremely effective for improvement of strength of the investigated alloy in addition to the grains having parallel orientation to the extrusion direction. Furthermore, it is noteworthy that the elongation reaches more than 30% and is much higher than that of as-received specimen, though the specimen ECAE-processed at 448 K exhibits high strength with low strain hardening. Consequently, an application of severe warm working like ECAE processing at low temperatures to AZ61 alloy makes it possible to achieve both high strength and high ductility.

4. Discussion

4.1. Grain size dependency of flow stress

Generally, yield stress of polycrystalline metals is well known to depend on its grain size, according to Hall–Petch relation. Fig. 7 shows the grain size dependencies of flow stresses of ECAE-processed AZ61 alloy specimens and the specimens annealed after ECAE processing. The AZ31 alloy specimens annealed after ECAE processing were indicated for comparisons. Flow stresses at strain of 2% were utilized instead of 0.2% proof stresses because it was difficult to measure the 0.2% proof stress of 4-pass ECAE-processed specimens. All the specimens show the clear grain size dependencies of flow stress. However, flow stresses of as-received AZ61 alloy specimen and the specimen ECAE-processed at 573 K indicated by open circle in the figure deviate upward from a straight line because these specimens have the texture, from the specimens ECAE-processed at 448–523 K in which the basal plane is mainly oriented parallel to the extrusion direction as shown in Fig. 5. The slope of the linear line, namely Hall–Petch coefficient, is about 0.15 MPa $m^{1/2}$, which is close to a value for various magnesium alloys reported by Koike et al. [17]. The flow stresses of the annealed AZ61 alloy specimens are 30 MPa higher than those of AZ31 annealed specimens. This would be caused by solution hardening. Furthermore, 4-pass ECAE-processed AZ61 alloy specimens show higher flow stress by about 50 MPa than the annealed AZ61 alloy specimens, as a result of dynamic precipitation of fine β phase. Thus, fine precipitates are also significantly effective for strength of the investigated alloy as well as grain refinement.

4.2. Slip systems

The high elongation appears with low strain hardening in ultra fine-grained AZ61 alloy obtained through the low temperature ECAE processing. The results are different from previously reported highly ductile AZ31 magnesium alloys, which show low yield strength and high strain hardening [4–10]. Hence, operation of some peculiar deformation mechanisms is expected on the ductility of the investigated alloy. In the following section, the reasons

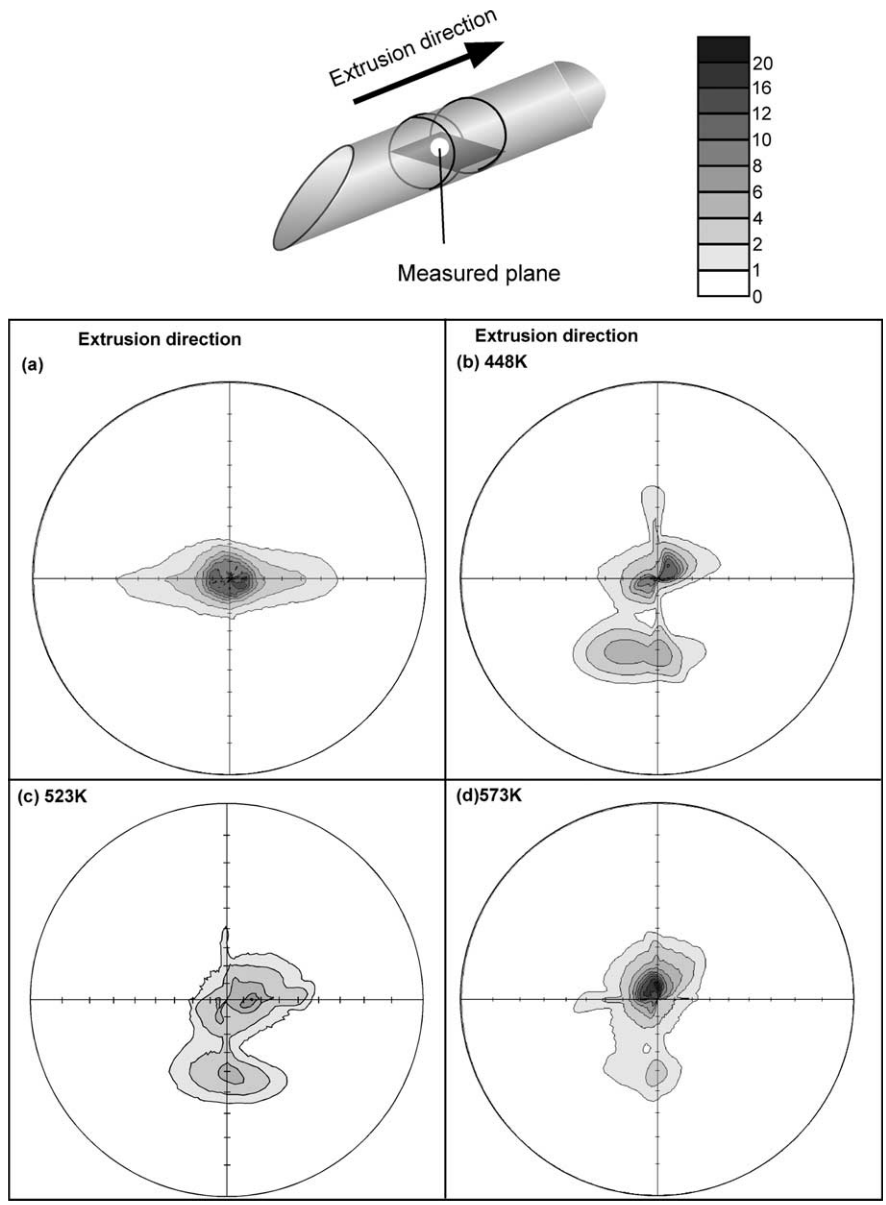

Fig. 5. 0002 pole figures of (a) as-received specimen, and ECAE specimens processed at (b) 448, (c) 523 and (d) 573 K.

for high ductility of the AZ61 alloy specimen ECAE-processed at 448 K are discussed.

Generally, it is said that only basal slip is active in deformation of magnesium at room temperature. However, basal slip has only two independent slip modes, which cannot accommodate the deformation along *c*-axis. Therefore, operation of other slip systems, i.e. non-basal slip, is required for high ductility of the magnesium alloys. TEM observations of the 448 K-ECAE-processed specimen deformed to 4% were carried out in order to investigate the active slip systems during tensile deformation. The observations were performed using a two-beam diffraction method. The result is shown in Fig. 8. The incident electron beam was aligned parallel to the $\langle 2\bar{1}\bar{1}0\rangle$ direction. Accordingly, the dislocation in the basal slip system appears parallel to the basal plane trace, whereas other dislocations are in non-basal slip systems. Some dislocations in non-basal slip system are visible in grain interior in addition to those in the basal slip system when the diffraction vector g is adapted to $0\bar{1}1\bar{1}$ diffraction. On the other hand, all dislocations are invisible when 0002 diffraction is excited, indicating that they have a Burgers vector according to $g \cdot b$ criterion. Koike et al. [11] reported activity of non-basal slip in 2%-elongated AZ31 alloy sample, and proposed that the non-basal slip is induced by compatibility stress that operates to maintain continuity at grain boundary. Furthermore, Kobayashi et al. [13] reported that non-basal slip operates in the region within 4 μm from the grain boundary. In other word, non-basal slip can operate in the whole interior of a grain when grain size is less than 8 μm. The

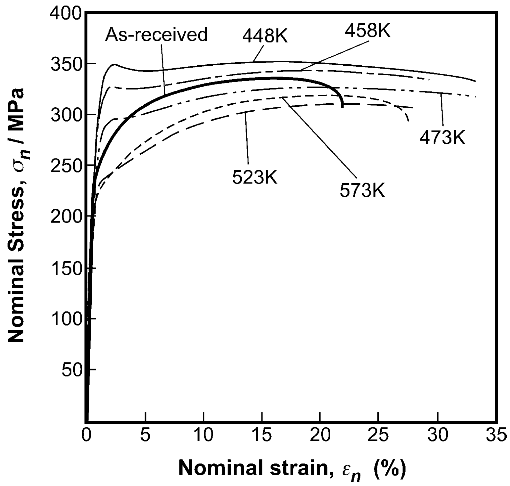

Fig. 6. Nominal stress–nominal strain curves of as-received specimens and ECAE-processed specimens. Temperatures given in figure indicate the ECAE processing ones.

annealed AZ61 alloy specimens having different grain sizes were tensile tested at room temperature at the strain rate of $1\times10^{-3}\ s^{-1}$ in order to appreciate the effect of grain size on ductility. Fig. 9 shows the correlation between grain size and elongation. The specimens having the grain size below 8 μm exhibit high elongation of about 33%, while the elongation of the specimen with the grain size of 30.3 μm is merely 21%. Thus, activity of non-basal slip near grain boundaries would be also helpful for the improvement of ductility of the present ECAE specimens. However, it would be difficult to provide an extra large elongation of 67% as described later only by an activity of the slip deformation. Therefore, additional deformation mechanisms such as twinning and GBS would operate as occurred in AZ31 alloy sample.

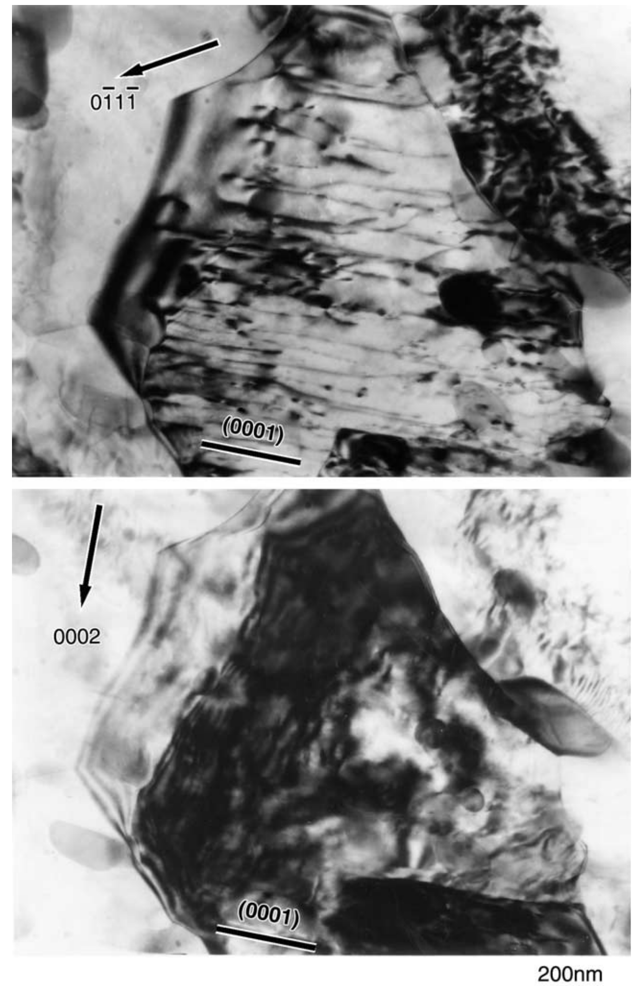

Fig. 8. TEM micrographs showing the occurrence of non-basal slip in ECAE specimen processed at 448 K. The specimen is tensile tested up to 4% strain. Diffraction vector g is indicated in the figure.

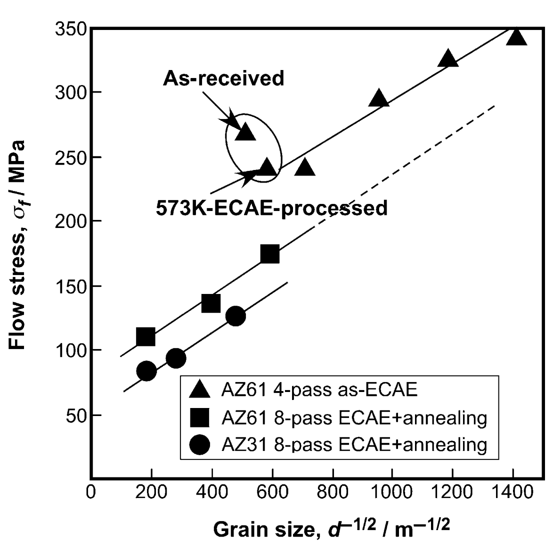

Fig. 7. Comparisons of grain size dependencies of flow stresses at strain of 2%.

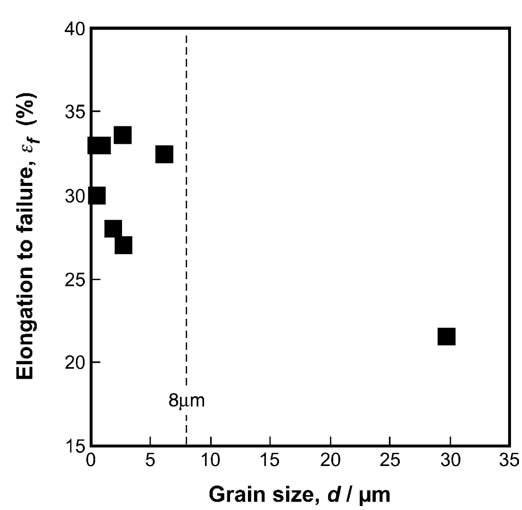

Fig. 9. Correlation between grain size and elongation in the investigated alloys.

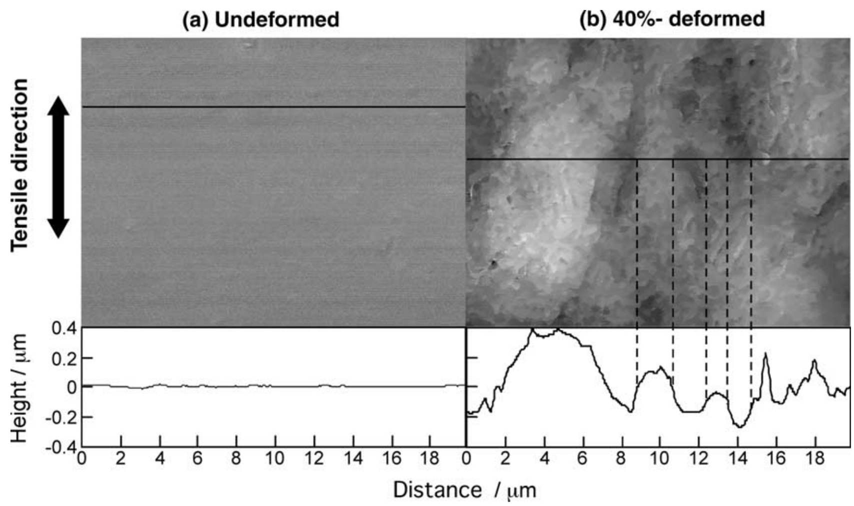

Fig. 10. Laser microscopic images (top) and sectional profiles (bottom) of undeformed specimen (left) and specimen deformed to 40% at RT under a strain rate of 1×10^{-5} s^{-1} (right). Contrast in the laser microscopic images is caused by the difference in height of the observed surface.

4.3. Grain boundary sliding

Fig. 10 shows laser microscopic images and sectional profiles along a line in the images of (a) undeformed and (b) 40%-deformed specimens. The undeformed specimen has quite smooth surface with an average roughness of about 0.02 μm. After 40%-deformation, the roughness of about 0.2–0.4 μm with steep steps appears on the specimen surface. It seems that the locations of the steps correspond to grain boundaries. This suggests the occurrence of GBS at room temperature. In addition, the step widths shown in Fig. 10(b) are apparently larger than the grain size of the as-ECAE-processed specimen shown in Fig. 3. This may indicate that the GBS occurs aggregately, not individually. Koike et al. [12] reported that the GBS in the AZ31 alloy having average grain size of 8 μm occurs even at room temperature and the ratio of the strain by GBS to total strain is about 8% at room temperature. In the present study, exact GBS-contributing strain could not be measured because the grains slide aggregately at grain boundaries. However, as shown in Fig. 10, the width of the steps are in the range from 1 to 2 μm and are remarkably less than the grain size of the specimen used by Koike et al. From the result, considerable GBS is considered to be responsible for the deformation even at room temperature.

4.4. Thermally activated process

The specimen ECAE-processed at 448 K exhibits high elongation in addition to high strength. Plastic flow accompanying low strain hardening as shown in Fig. 6 suggests possibility of softening by thermal activation process. Fig. 11 shows stress–strain curves of the 448 K-specimen tensile-tested under various strain rates. Elongation increases with a decrease in strain rate, i.e. the specimen tested at a strain rate of 1×10^{-5} s^{-1} exhibits an extra large elongation of 67% even at room temperature,

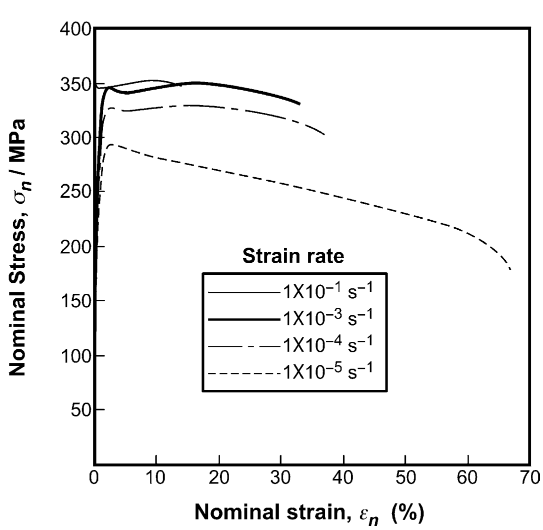

Fig. 11. Nominal stress–nominal strain curves of specimens ECAE-processed at 448 K under various strain rate.

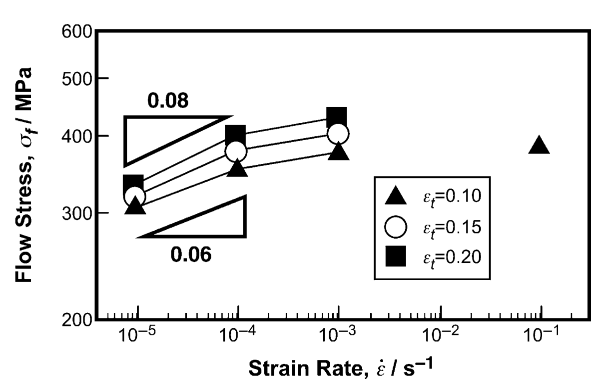

Fig. 12. Strain rate dependencies of flow stresses under various true strain. Strain rate sensitivity exponent, *m*-values, are also indicated in the figure.

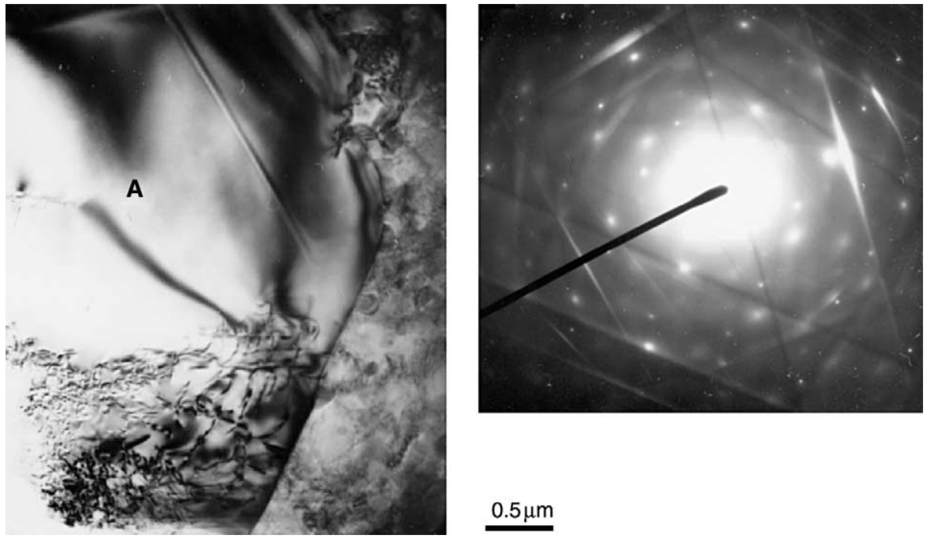

Fig. 13. TEM photograph (left) of specimen deformed by 20% at a strain rate of $1\times10^{-5}\ s^{-1}$ and diffraction pattern (right) from region A indicated in the left image.

while the elongation of the specimen tested at a strain rate of $1\times10^{-1}\ s^{-1}$ is merely 14%. It can be seen from Fig. 11 that the plastic flow stresses also depend on the strain rate. The strain rate dependence of flow stress at various true strain levels is shown in Fig. 12. The true stress at each true strain is used as the value of flow stress. In a low strain rate region, strain rate sensitivity exponent, m-values, is 0.06–0.08, which is relatively high values for deformation at room temperature. These facts suggest that thermally activated process such as dynamic recovery would have participated in the deformation process even at room temperature. Fig. 13 shows a TEM photograph of the specimen deformed by 20% at a strain rate of $1\times10^{-5}\ s^{-1}$. Any dislocations are invisible in this grain, and Kikuchi bands are clearly observed. Thus, some grains including no dislocations exist even in the specimen deformed by large elongation of 20%. This would be an evidence of the above suggestion. Furthermore, it is noted that any twins cannot be observed in such specimen. Therefore, it can be concluded that the high elongation of the investigated specimen with fine grains is provided by non-basal slip, GBS and dynamic recovery in addition to dislocation slip on basal plane.

5. Summary

Commercial extruded AZ61 magnesium alloy bars were subjected to 4-pass ECAE processing at 448–573 K. Then the microstructures were observed, and tensile properties of the ECAE processed specimens at RT were investigated. After ECAE processing at 448 K, extremely fine grains with average grain size of 0.5 μm are formed by dynamic recrystallization being attributable to dislocation pileups that occur in the vicinity of dynamically—precipitated β phase particles of less than 100 nm diameter. Such specimens show high tensile strength of 350 MPa with low strain hardening, and elongation reaches 33% at a strain rate of $1\times10^{-3}\ s^{-1}$. Furthermore higher elongation of 67% is attained at a strain rate of $1\times10^{-5}\ s^{-1}$. Dislocation slip on non-basal plane, dynamic recovery and grain boundary sliding in addition to basal slip can lead to extremely high elongation in fine-grained AZ61 alloy specimen.

Acknowledgements

The present study is supported by COE Program for the 21st Century ‘Creation of Hybridized Materials with Super-Functions and Formation of International Research and Education Center’ from Nagaoka University of Technology. The authors would like to thank to Prof. K. Yatsui, Prof. W. Jiang, Prof. H. Suematsu and Dr T. Suzuki of Extreme Energy-Density Research Institute of Nagaoka University of Technology for their support in X-ray diffraction analysis.

References

[1] D.V. Wilson, The ductility of polycrystalline magnesium below 300 K, J. Inst. Metals 98 (1970) 133–143.
[2] G. Sambasiva Rao, Y.V.R.K. Prasad, Grain boundary strengthening in strongly textured magnesium produced by hot rolling, Metall. Trans. A 13A (1982) 2219–2226.
[3] M. Mabuchi, Y. Chino, H. Iwasaki, T. Aizawa, K. Higashi, The grain size and texture dependence of tensile properties in extruded Mg–9Al–1Zn, Mater. Trans. 42 (2001) 1182–1189.
[4] H. Watanabe, T. Mukai, S. Kamado, Y. Kojima, K. Higashi, Mechanical properties of Mg–Y–Zn alloy processed by equal-channel-angular extrusion, Mater. Trans. 44 (2003) 463–467.

[5] T. Mukai, M. Yamanoi, H. Watanabe, K. Higashi, Ductility enhancement in AZ31 magnesium alloy by controlling its grain structure, Scripta. Mater. 45 (2001) 89–94.

[6] W.J. Kim, C.W. An, Y.S. Kim, S.I. Hong, Mechanical properties and microstructures of an AZ61 Mg alloy produced by equal channel angular pressing, Scripta. Mater. 47 (2002) 39–44.

[7] Y. Yoshida, L. Cisar, S. Kamado, Y. Kojima, Effect of microstructural factors on tensile properties of an ECAE-processed AZ31 nagnesium alloy, Mater. Trans. 44 (2003) 468–475.

[8] Y. Yoshida, K. Arai, S. Itoh, S. Kamado, Y. Kojima, Superplastic deformation of AZ61 magnesium alloy having fine grains, Mater. Trans. 45 (2004) 2537–2541.

[9] W.J. Kim, S.I. Hong, Y.S. Kim, S.H. Min, H.T. Jeong, J.D. Lee, Texture development and its effect on mechanical properties of an AZ61 Mg alloy fabricated by equal channel angular pressing, Acta Mater. 51 (2003) 3293–3307.

[10] S.R. Agnew, J.A. Horton, T.M. Lillo, D.W. Brown, Enhanced ductility in strongly textured magnesium produced by equal channel angular processing, Scripta. Mater. 50 (2004) 377–381.

[11] J. Koike, T. Kobayashi, T. Mukai, H. Watanabe, M. Suzuki, K. Maruyama, K. Higashi, The activity of non-basal slip systems and dynamic recovery at room temperature in fine-grained AZ31B magnesium alloys, Acta Mater. 51 (2003) 2055–2065.

[12] J. Koike, R. Ohyama, T. Kobayashi, M. Suzuki, K. Maruyama, Grain-boundary sliding in AZ31 magnesium alloys at room temperature to 523 K, Mater. Trans. 44 (2003) 445–451.

[13] T. Kobayashi, J. Koike, Y. Yoshida, K. Kamado, M. Suzuki, K. Maruyama, Y. Kojima, Grain size dependence of active slip systems in an AZ31 magnesium alloy, J. Jpn Inst. Metals 67 (2003) 149–152.

[14] L.G. Schulz, A direct method of determining preferred orientation of a flat reflection sample using Geiger counter X-ray spectrometer, J. Appl. Phys. 20 (1949) 1030–1033.

[15] J. Kaneko, M. Sugamata, M. Numa, Y. Nishikawa, H. Takada, Effect of texture on the mechanical properties and formability of magnesium wrought materials, J. Jpn Inst. Metals 64 (2000) 141–147.

[16] S. Kleiner, P.J. Uggowitzer, Mechanical anisotropy of extruded Mg–6%Al–1%Zn alloy, Mater. Sci. Eng. A 379 (2004) 258–263.

[17] J. Koike, K. Kobayashi, Microstructure, deformation and diffusion of magnesium, Procedings of a Subcommittee Symposium of the Japan Institute of Metals “Fundamentals of Magnesium and Industrial Applications”, The Japan Institute of Metals, Sendai, 2001, pp. 1–3.